

Topological thermal instability and length of proteins

Raffaella Burioni and Davide Cassi

*Dipartimento di Fisica and INFN, Università di Parma,
Parco Area delle Scienze 7A, 43100 Parma, Italy*

Fabio Cecconi and Angelo Vulpiani

*Dipartimento di Fisica and INFN (UdR and SMC) ,
Università di Roma La Sapienza, P.le A. Moro 2, 00185 Roma, Italy*

Abstract

We present an analysis of the effects of global topology on the structural stability of folded proteins in thermal equilibrium with a heat bath. For a large class of single domain proteins, we computed the harmonic spectrum within the Gaussian Network Model (GNM) and determined the spectral dimension, a parameter describing the low frequency behaviour of the density of modes. We find a surprisingly strong correlation between the spectral dimension and the number of amino acids of the protein. Considering that larger spectral dimension value relate to more topologically compact folded state, our results indicate that for a given temperature and length of the protein, the folded structure corresponds to the less compact folding compatible with thermodynamic stability.

INTRODUCTION

The role of geometry has recently been considered as a factor of primary importance for the study of several physical properties of proteins and other biological macromolecules. In particular, since the topology of folded states is known to influence the folding properties of the protein [1, 2, 3, 4, 5, 6, 7, 8], a great deal of work has been devoted to the study of those theoretical aspects which describe the networks of links between amino acids in folded proteins. [9, 10, 11]. Furthermore, relevant features of protein conformations seem to follow the geometrical principles of the optimal packing problem [12, 13] and mathematical concepts from graph theory have been interestingly applied to identify flexible and rigid regions of folded states [14].

Starting from the primary, linear structure (the sequence of amino acids), a protein evolves during the folding process until it reaches a final state (native state) whose geometrical shape is crucial to the function of the protein itself. However, the problem of the geometrical arrangement of proteins in their native states cannot be regarded as purely static issue. Indeed, a massive accumulation of experimental data collected from X-ray, NMR and neutron spectroscopy, has revealed that protein native states are rather dynamic structures where amino acids constantly move around their equilibrium positions. This motion, crucially involved in protein functions [15, 16], is usually examined and investigated through normal modes analysis (NMA) [17] or essential dynamics [18]. However, the study of collective motions of large scale proteins is generally difficult due to limited access to realistic all-atoms NMA [19] and simplified or approximate approaches are usually welcome. Tirion [20] first proposed the possibility of replacing, in protein normal mode computations, complicated empirical potentials by Hookian pairwise interactions depending on a single parameter. This approach stems from the observation that low-frequency dynamics, which are mainly associated with protein-domain motion, are generally insensitive to the finer details of atomic interactions. Much of the subsequent literature [21, 22, 23, 24, 25, 26] has confirmed the success of simple harmonic models in the study of slow vibrational dynamics of large biological macromolecules, and they have become a viable alternative to heavy and time-consuming all-atoms NMA. This success result from the striking agreement of predictions with experiments, the presence of few adjustable parameters and the fast and easy numerical implementation on computers and fast result production. For these reasons

harmonic models are also utilized for the systematic analysis of large data sets of proteins.

The topological stability of macromolecules is far from being a pure mechanical problem as it closely involves thermodynamics. Indeed, the relevant thermodynamic potential that must be minimized in order to find the stable configuration is not energy, but free energy. This is due to the interaction with the environment (schematized as a thermal bath) which is generally not negligible, especially for biological macromolecules that have a stable phase in a solvent. In particular, water is a very efficient medium for the transfer of thermal energy at microscopic scales (i.e. oscillations and molecular rotations).

With these considerations in mind, in this work we apply NMA to investigate the influence of the global native state topology on the thermal stability of proteins.

Vibrational thermal instability is a well-known topic of study in solid state physics. Since the initial classical analysis of Peierls [27], it has been recognized that equilibrium with a thermal bath can dramatically influence the possible topological arrangement of large geometrical structures. Up to now, the most striking consequence of Peierls' instability has concerned low-dimensional crystals: for one and two-dimensional lattices the mean square displacement of a single atom at finite temperature diverges in the thermodynamic limit, i.e. with an increasing number of atoms. When the displacement exceeds the order of magnitude of the lattice spacing, the topological arrangement of the lattice is unstable and the crystal becomes a liquid. For real structures, formed by a finite number of units and far from the thermodynamic limit, the divergence sets a maximal stability size, which is negligible for one-dimensional lattices and typically mesoscopic for two-dimensional lattices.

However, thermal instability is present not only in crystals but also in structurally inhomogeneous systems, such as glasses, fractals, polymers and non crystalline structures. Here, the problem is much more complex. Generalizing the Peierls approach to mesoscopic disordered structures, we are able to apply this kind of argument to the thermal stability of macromolecules. In this article we describe how this can be done in the case of proteins; we predict the existence of a critical stability size depending on a global topological parameter (the spectral dimension) and compare our predictions with experimental data.

THEORY

In a recent paper [28] generalizing the Peierls' result, we showed that a thermodynamic instability also appears in inhomogeneous structures and is determined by the spectral dimension \bar{d} . The parameter \bar{d} [29] is defined according to the asymptotic behaviour of the density of harmonic oscillations at low frequencies. More precisely, using $g(\omega)$ to denote the density of modes with frequency ω , then

$$g(\omega) \sim \omega^{\bar{d}-1} \quad (1)$$

for $\omega \rightarrow 0$. The spectral dimension is the most natural extension of the usual Euclidean dimension d to disordered structures as far as dynamical processes are concerned. It coincides with d in the case of lattices, but in general, it can assume non-integer values between 1 and 3. The spectral dimension represents a useful measure of the effective connectedness of geometrical structures at large scales, because large values of \bar{d} correspond to high topological connectedness. Moreover, it characterizes not only harmonic oscillations, but it also relates to diffusion, phase transitions and electrical conductivity, allowing a variety of both experimental and numerical methods for its determination [30, 31]. The relevance of \bar{d} in connection with the anomalous density of vibrational modes in proteins has also been considered in refs.[32, 33].

In the case of thermal instability, we demonstrated that, for $\bar{d} \geq 2$, the mean square displacement $\langle r^2 \rangle$ of a structural unit (being an atom, a molecule or a supra-molecular structure according to the studied case) of a system composed of N elements, diverges in the limit $N \rightarrow \infty$. Using T to denote the temperature of the heat bath, with k_B the Boltzmann constant, and with γ the interaction energy scale, the divergence is given by the asymptotic law:

$$\langle r^2 \rangle \sim \frac{k_B T}{\gamma} N^{2/\bar{d}-1} \quad (2)$$

when $\bar{d} < 2$. When $\bar{d} = 2$, the mean square displacement diverges logarithmically, $\langle r^2 \rangle \sim k_B T / \gamma \ln(N)$, as in the case of the Peierls' result for a two dimensional crystal. Notice that the divergence in $\langle r^2 \rangle$ is only determined by \bar{d} . Now, at any given temperature T , there will exist a threshold value $N(T)$ beyond which $\langle r^2 \rangle^{1/2}$ exceeds the typical spacing between the nearest neighbors, making the solid structure unstable. Therefore at large enough values of N , the solid will experience a structural reorganization which can lead

either to a homogeneous liquid phase at sufficiently high temperatures or to a disordered 3-dimensional solid, which is homogeneous on a large scale and inhomogeneous at a small scale. In general, the threshold values of N are very small with respect to the typical order of magnitude of macroscopic systems, being rather comparable to the size of large complex macromolecules such as biopolymers.

This poses an intriguing question concerning proteins. Indeed, to exploit their biological function proteins must keep a specified geometrical and topological arrangement and cannot afford any, even partial, large scale geometrical fluctuations such as it happen, to swollen polymeric chains in a good solvent [34]. This makes thermodynamical stability crucial and suggests a possible correlation between the spectral dimension and the length of protein chains.

Vibrational stability in proteins has been analysed with the Gaussian network model (GNM), proposed by Bahar et al. [35] and widely applied because it yields results in agreement with principal X-ray spectroscopy experiments. This approach generally considers proteins as elastic networks, whose nodes are the positions of the alpha-carbons (C_α) in the native structure and the interactions between nodes are assimilated to harmonic springs. The only information required to implement the method is the knowledge of the native structure, and two parameters are introduced, the spring constant and the interaction cut-off, which, however turn out to be related whenever the model is applied to fit experimental data. The GNM can be defined by the quadratic Hamiltonian

$$H = \sum_i^N \frac{\mathbf{P}_i^2}{2m} + \frac{\gamma}{2} \sum_{ij} \Delta_{ij} (\delta \mathbf{r}_i - \delta \mathbf{r}_j)^2 \quad (3)$$

where the first term is the kinetic energy of the system, γ being the strength of the springs that are assumed homogeneous, \mathbf{R}_i and $\delta \mathbf{r}_i$ indicating the equilibrium position and the displacement with respect to \mathbf{R}_i of the i -th C_α atoms. The model is eventually defined by the contact matrix Δ with entries: $\Delta_{ij} = 1$ if the distance $|\mathbf{R}_i - \mathbf{R}_j|$ between two C_α 's, in the native conformation, is below the cutoff R_0 , while is 0 otherwise.

The harmonic spectrum for each structure is given by the set of eigenvalues $\{\omega_1, \dots, \omega_N\}$ of the Kirchoff matrix (or valency-adjacency matrix) $\Gamma_{ij} = -\Delta_{ij} + \delta_{ij} \sum_{l \neq i} \Delta_{il}$,

Notice that the first eigenvalue ω_1 vanishes and corresponds to the constant eigenvector related to the trivial uniform translation.

The comparison between experimental data and GNM results is obtained via the X-ray

crystallographic B -factors, measuring the mean square fluctuation of C_α atoms around their native positions

$$B_i(T) = \frac{8\pi^2}{3} \langle \delta \mathbf{r}_i \cdot \delta \mathbf{r}_i \rangle$$

with $\langle \cdot \rangle$ indicating the thermal average. In the GNM approximation, this average is easily carried out, because amounts to a Gaussian integration, and B -factors can be expressed in terms of the diagonal part of the inverse of the matrix Γ [35]:

$$\langle \delta \mathbf{r}_i \cdot \delta \mathbf{r}_j \rangle = \frac{3k_B T}{\gamma} [\Gamma^{-1}]_{ij}$$

The knowledge of the eigenvectors and eigenmodes of matrix Γ allows to compute the GNM B -factors also through formula

$$B_i(T) = \frac{8\pi^2 k_B T}{\gamma} \sum_k \frac{|u_i(k)|^2}{\omega_k^2}$$

where i is the residue index, the sum runs over all non-zero frequencies ω_i and $u_i(k)$ indicates the i -th component of the k -th eigenmode.

The comparison with crystallographic data is crucial for setting the correct values of the parameters R_0 and γ . (see. Methods and Results).

METHODS

We present a GNM harmonic analysis performed over the dataset of protein native structures with different sizes downloaded from the Brookhaven Protein Data Bank. The purpose of the analysis is basically to investigate whether there exists a correlation between the spectral dimension of native structures and the length of natural occurring proteins and, if so, to verify whether the correlation can be explained in terms of the above mentioned stability criterion determined by equation (2).

Our representative statistical sample, listed in Tables I and II, was selected according to the following criteria. First, we only considered proteins with a stable large scale geometry. This excludes multiple domains proteins, where domains can undergo relative motion giving rise to larger geometrical fluctuations. Moreover, we considered only proteins not binded to fragments of DNA, RNA or other substrates because such structures cannot be described

with sufficient accuracy in terms of simple harmonic model with only two effective parameters. Finally, we choose proteins covering uniformly a wide length interval ranging from 100 to 3600 to test our prediction.

The diagonalization of the Kirchhoff matrix Γ to obtain its eigenvalues $\{\omega_1^2, \dots, \omega_n^2\}$ and eigenvectors has been performed with the standard numerical packages [36].

The value of the interaction cutoff for generating the contact matrix Δ has been set to $R_0 = 7\text{\AA}$ as customarily in such kind of studies. The cutoff choice, which affects the overall GNM performance, is generally tested through the correlation coefficient ρ [37]

$$\rho = \frac{\sum_i (B_i - \langle B \rangle)(X_i - \langle X \rangle)}{\sqrt{\sum_{ij} (B_i - \langle B \rangle)^2 (X_j - \langle X \rangle)^2}} \quad (4)$$

between experimental (X_i) and theoretical (B_i) B-factors. The sum runs over the number of protein residues, and $\langle X \rangle$, $\langle B \rangle$ indicate the average values. Our data set contains only those protein structures with a coefficient ρ greater than 0.5 (see last column of Tables I and II.) this should, in principle, ensure that GNM correctly reproduces C_α fluctuations for each selected protein. However since we shall study two different cutoffs, we decided to include even those few structures, such as 9RNT, 1A47, and 1CDG, that have a $\rho > 0.5$ for one cutoff and $\rho < 0.5$ for the other one. The few instances of the agreement between B-factors from GNM and crystallography are shown in figure 1, where we display the best and the worst cases with respect to the coefficient ρ .

For each protein, the optimal value of the spring constant γ was obtained through a least-square fitting to the experimental B-factors expressed by formula

$$\frac{k_B T}{\gamma} = \frac{1}{8\pi^2} \frac{\sum_i B_i X_i}{\sum_i B_i^2} \quad (5)$$

The values of $k_B T/\gamma$, besides being an essential ingredient for the real application of GNM method, are also an indication of the protein global flexibility and allows for a direct comparison among all the considered structure.

The spectral dimension \bar{d} was estimated via a power-law fitting of the low frequency behaviour of the cumulated density of modes $G(\omega)$, namely the integral of $g(\omega)$. Indeed, due to relation (1), $G(\omega) \sim \omega^{\bar{d}}$ at small arguments (see Fig. 2). The harmonic spectrum, obtained within the GNM, for three proteins with sizes, small, medium and large, respectively is plotted in figure 2, where low-frequency regions clearly exhibit the power law behavior whose exponent is the spectral dimension \bar{d} .

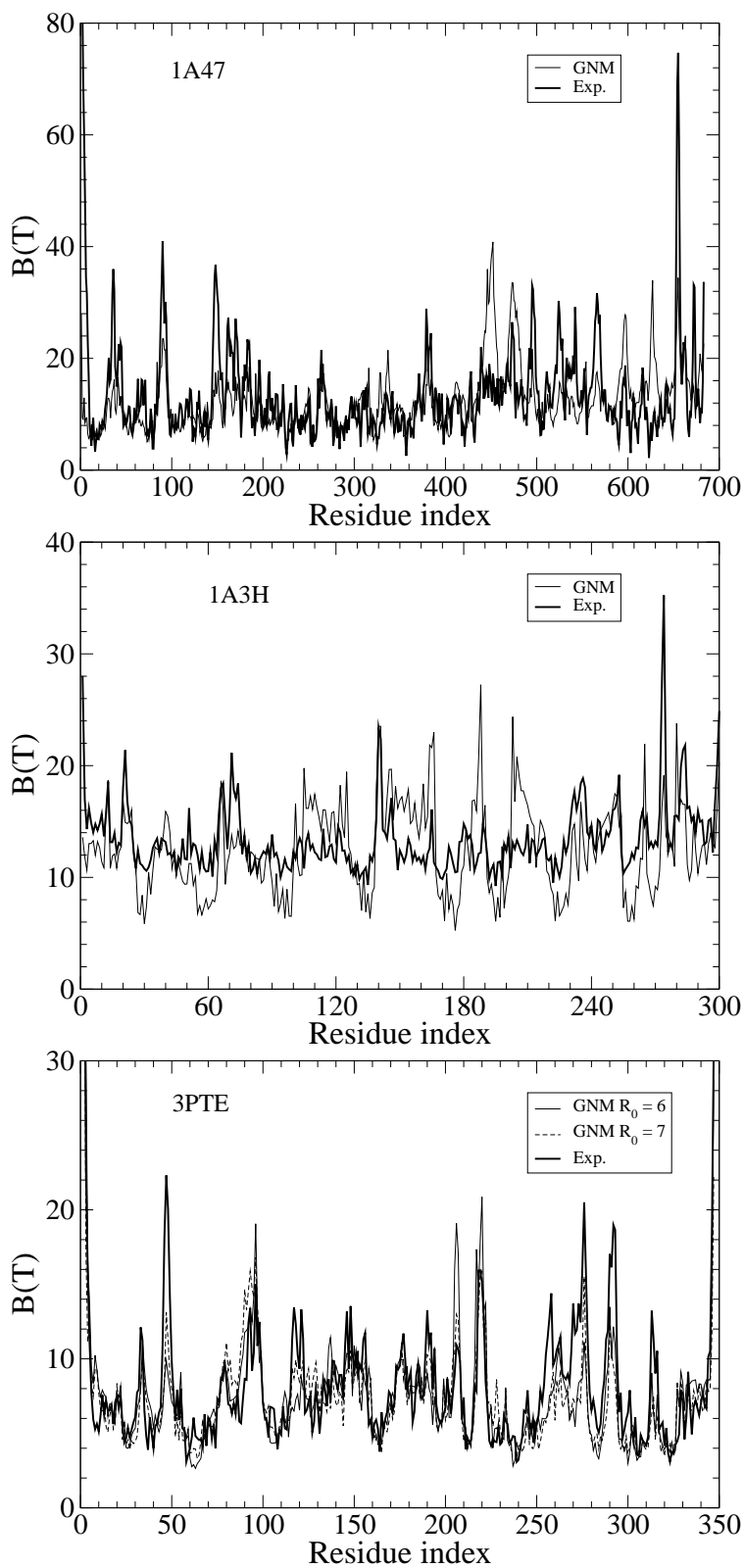


FIG. 1: Comparison between experimental B-factors and mean square fluctuations of C_α by GNM, for the structures 1A47 (lowest correlation) and 3PTE (highest correlation) at cutoff $R_0 = 7\text{\AA}$, and structures 9RNT (lowest correlation) and 3PTE (highest correlation) at cutoff $R_0 = 6\text{\AA}$. Heavy solid line refers to crystallographic data, while thin and dashed lines refers to GNM approximation.

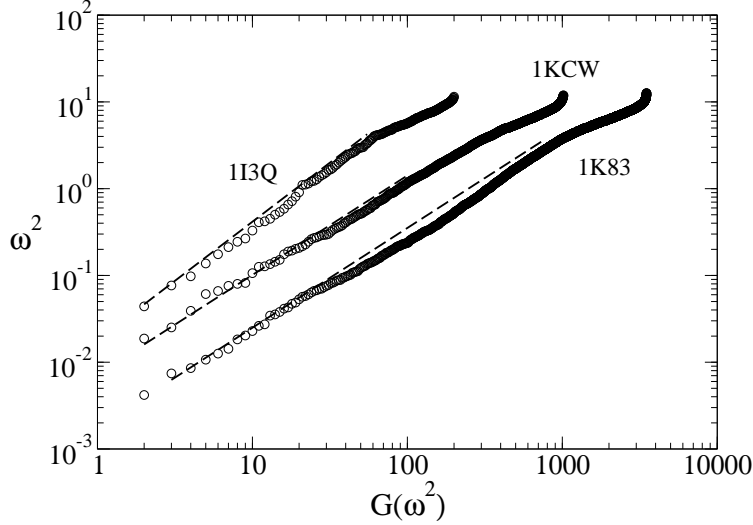


FIG. 2: Log-log plot of GNM-harmonic spectrum referred to three proteins with different sizes, 1I3Q ($N=200$), 1KCW ($N=1017$) and 1K83 ($N=3494$). On vertical axis, we report the cumulated distribution $G(\omega)$ of vibrational modes. Low frequencies regions clearly exhibit a power-law behaviour, and dashed lines indicates the best-fits of the power-law whose exponent is the spectral dimension.

RESULTS AND DISCUSSION

Our statistical analysis for the whole dataset of proteins and cutoffs $R_0 = 7\text{\AA}$ is summarized in Table I, where we report the spectral dimension and its corresponding error, the estimate for $k_B T/\gamma$, and finally the correlation coefficient. To test the robustness of our results, we have repeated the same analysis at a slightly different cutoff, namely at $R_0 = 6\text{\AA}$, which yields a smaller but still good correlation between experimental and theoretical B-factors (Tab. II). Errors on \bar{d} -values, in both tables, were estimated to cover the uncertainty due to the choice of the fitting region for the power-law, because the slope of the linear-fitting (see Fig. 2) can change even sensibly upon varying this region. Furthermore, error bars take into account also correlation data (ρ) which indicates how GNM can faithfully reproduce the low-energy deformations of a given protein structure.

The relationship (2) establishes a rather strong constraint between the spectral dimension and the maximum size N_{max} of a protein can afford. Since, the stability is supposed to fail when the fluctuation $\langle r^2 \rangle^{1/2}$ becomes of the same order of magnitude of the mean distance

between non consecutive amino acids (about 7 \AA), one can assume that

$$\frac{2}{\bar{d}} = 1 + \frac{b}{\ln(N_{max})}. \quad (6)$$

The proportionality constant b depends on the mean amino acid spacing, on the spring elastic constant γ and temperature T . However, this dependence is expected to be very weak (i.e. only logarithmic) and this allows for a comparison of different proteins without the computation of the specific parameters. It should be stressed that equation (6), being based uniquely on thermodynamics stability, can be actually regarded as an upper bound prediction only.

Figure verifies the prediction drawn from the thermodynamical stability argument and shows the final result of our analysis. We plot the quantity $2/d$ versus $1/\ln(N)$ as suggested by relation (6): indeed, if Eq. (6) holds, we should obtain a straight line crossing the y-axis at 1 for zero abscissa. As matter of fact, our data are well fitted by a straight line, but, with an offset with respect to the equation (6)

$$\frac{2}{\bar{d}} = a + \frac{b}{\ln(N)}. \quad (7)$$

For case of a cutoff $R_0 = 7 \text{ \AA}$, best-fit values of the parameters are $a = 0.63$, $b = 2.61$, with a correlation coefficient 0.73. For the cutoff $R_0 = 6 \text{ \AA}$, we obtained the values $a = 0.63$, $b = 3.40$. with a correlation 0.72. Interestingly, the linear behaviour predicted by Eq. (6) is confirmed for two different cutoffs with a correlation larger than 0.7, providing a strong evidence of the robustness of the result.

CONCLUSIONS

We applied the Gaussian Network Model (GNM) to investigate the influence of native state topology on thermodynamical stability for a set of folded proteins with a very different sizes, ranging from 100 to 3600. Employing the GNM is appropriate in this type of study because such a model correctly accounts for the topological features of the native protein conformations. Our results show that the spectral dimension \bar{d} , which is sensitive to the large scale topology of a geometrical structure, is one parameter governing the low-energy fluctuations of a given protein structure. As a consequence, one can derive an instability criterion for proteins, based only on topological considerations, which is the analogous of

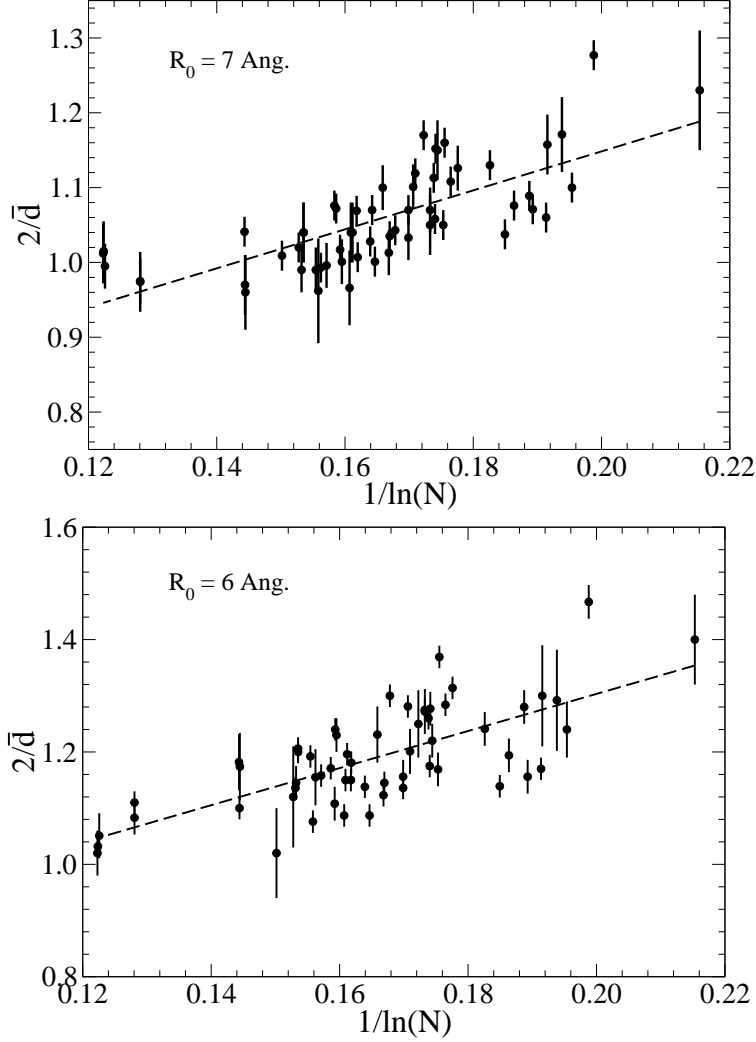


FIG. 3: Linear plot showing the dependence of the spectral dimension on protein size. The dashed line, indicating the behaviour 7, is a best fit with a correlation coefficient 0.73 and 0.72 for cutoffs 7\AA and 6\AA respectively.

Peierls' criterion developed for ordered crystalline structures. The criterion easily predicts a non-trivial logarithmic dependence of the spectral dimension on the length of a protein. This further confirms the lack of universality for the spectral dimension of proteins [32], an issues already addressed in previous studies [24]. We verified that such a logarithmic dependence is really observed, within statistical and systematic errors, for the whole set of selected proteins. Furthermore, the dependence is robust because it applies even with alteration of the interaction cutoff which is the most critical parameter to the GNM applicability. We can conclude that the relation between spectral dimension and length of proteins is

not an artifact due to a particular cutoff choice, providing that a significant correlation is maintained between experimental and theoretical B-factors. We verified that, at a larger cutoff, the scaling behaviour (7) is preserved, although the spectral dimension grows due to the increase in the average connectivity of the elastic network.

The result expressed by Eq. (7) deserves some comments.

Equation (7) is in agreement with the upper bound represented by Eq. (6), supporting the relevance of topological thermal instability as a constraint to protein geometry. More importantly, not only is the upper bound satisfied, but the experimental points lie on a straight line parallel to the upper bound line of Eq. (6). This suggests a more fundamental role of topological stability: the protein tends to arrange topologically in such a way to reach the minimum value compatible with stability constraints. In other words, for any fixed length, it tends to the most swollen state which remains stable with respect to thermal fluctuations.

An interesting point is the meaning of the offset $a - 1$ which would be 0 according to Eq. (6). Its positive value could have different explanations, but its universal nature (it is a “protein-independent” because is a global shift) must be due to a very general mechanism. A rather obvious reason is the contribution of anharmonic interactions at finite temperatures; a more intriguing one could be an effective longer range interaction due to the presence of bound water molecules around the external amino acids, which could change the effective form of the interaction matrix Λ . This hypothesis is also suggested by the physical interpretation of b as an anomalous dimension exponent, typically related to a renormalized interactions [38]. However, the most intriguing evidence relies on the regression coefficient. Independently of the physical origin of b , its high value strongly supports the existence of a thermodynamic stability threshold, dependent on the topology of the folded state, for the size of proteins.

-
- [1] Gø N. and Scheraga H.A. On the Use of Classical Statistical Mechanics in the Treatment of Polymer Chain Conformation. *Macromolecules* 1976;9; 535-549.
 - [2] Plaxco K.W. ,Simons K.T. and Baker D. Contact order, transition state placement and the refolding rates of single domain proteins. *J. Mol. Biol.* 1999;277; 985-994.

- [3] Makarov D.E., Keller C.A., Plaxco K.W., Metiu H. How the folding rate constant of simple, single-domain proteins depends on the number of native contacts. *Proc. Natl. Acad. Sci. USA*, 2002;99; 3535-3539.
- [4] Riddle D.S., Grantcharova V.P., Santiago J.V., Alm E., Ruczinski I. and Baker D. Experiment and theory highlight role of native state topology in SH3 folding. *Nature Struct. Biol.* 1999;6; 1016-1024.
- [5] Baker D. A surprising simplicity to protein folding. *Nature* 2000;405; 39-42.
- [6] Clementi C., Nymeyer H. and Onuchic J.N. Topological and energetic factors: What determines the structural details of the transition state ensemble and "en-route" intermediates for protein folding? An investigation for small globular proteins. *J. Mol. Biol.* 1998;298; 937-953.
- [7] Klimov D.K., and Thirumalai D. Native topology determines force-induced unfolding pathways in globular proteins. *Proc. Natl. Acad. Sci. USA* 2000;97; 7254-7259.
- [8] Cecconi F., Micheletti C., Carloni P. and Maritan A. Molecular dynamics studies on HIV-1 protease drug resistance and folding pathways. *Proteins: Struct. Func. Gen.* 2001;43; 365-372.
- [9] Kabakcioglu A., Kanter I., Vendruscolo M. and Domany E. Statistical properties of contact vectors. *Phys. Rev. E* 2002;65; 041904.
- [10] Park K., Vendruscolo M. and Domany E. Toward an energy function for the contact map representation of proteins. *Proteins: Struct. Func. Gen.* 2000;40; 237-248.
- [11] Vendruscolo M., Dokholyan N.V., Paci E. and Karplus M. Small-world view of the amino acids that play a key role in protein folding *Phys. Rev. E* 2002;65; 061910.
- [12] Maritan A., Micheletti C., Trovato A. and Banavar J.R., Optimal shapes of compact strings. *Nature* 2000;406; 287-290.
- [13] Banavar J.R. and Maritan A. Geometrical approach to protein folding: a tube picture. *Rev. Mod. Phys.* 2003;75; 23-34.
- [14] Jacobs. D.J., Rader A.J., Kunh L.A., Thorpe M.F., Protein flexibility prediction using graph theory. *Proteins: Struct. Funct. Genet.* 2001;44; 150-165.
- [15] Frauenfelder H., Petsko G.A. and Tsernoglou D. Temperature dependent x-ray diffraction as a probe as of protein structural dynamics. *Nature* 1979;280; 558-563.
- [16] Frauenfelder H., McMahon B. Dynamics and functions of proteins: the search of general concepts. *Proc. Natl. Acad. Sci. USA* 1998;95; 4795-4797.
- [17] Karplus M. and McCammon J. Dynamics of Proteins: Elements and Functions. *Ann. Rev.*

- Biochem. 1983;53; 263-300.
- [18] Amadei A., Linssen A.B.M., Berendsen H.J.C., Essential dynamics of proteins. *Proteins: Struct. Func. Gen.* 1993;17; 412-425.
- [19] Levitt M., Sanders C. and Stern P.S. Protein normal-mode dynamics; trypsin inhibitor, crambin, ribonuclease, and lysozyme. *J. Mol. Biol.* 1985 ;181; 423-447.
- [20] Tirion M.M. Low-amplitude elastic motions in proteins from a single-parameter atomic analysis. *Phys. Rev. Lett.* 1996;77; 1905-1908.
- [21] Hinsen K. Analysis of domain motion by approximate normal mode calculations. *Proteins: Struct. Funct. Genetics* 1999;33; 417-429.
- [22] Bahar I., Atilgan A.R., Demirel M.C, Erman B. Vibrational dynamics of folded proteins: Significance of slow and fast motions in relation to function and stability. *Phys. Rev. Lett.* 1998;80; 2733-2736.
- [23] Atilgan A.R., Durell S.R., Jernigan R.L., Demirel M.C., Keskin O. and Bahar I. Anisotropy of fluctuation dynamics of proteins with an elastic network model. *Biophys. J.* 2001;80; 505-515.
- [24] Haliloglu T., Bahar I., Erman. B. Gaussian dynamics of folded proteins. *Phys. Rev. Lett.*1997;79; 3090-3093.
- [25] Micheletti C., Cecconi F., Flammini A., Maritan A. Crucial stages of protein folding through a solvable model: Predicting target sites for enzyme-inhibiting drugs. *Protein Sci.* 2002;11; 1878-1887.
- [26] Micheletti C., Lattanzi G., Maritan A. Elastic properties of proteins: insight on the folding processes and evolutionary selection of native structures. *J. Mol. Biol.* 2002;321; 909-921.
- [27] Peierls R.E. Bemerkung über Umwandlungstemperaturen. *Helv. Phys. Acta* 1934;7; S81-S83.
- [28] Burioni R., Cassi D., Fontana M.P., Vulpiani A. Vibrational thermodynamic instability of recursive networks. *Europhysics Lett.* 2002;58; 806-810.
- [29] Alexander S., Orbach R.L. Density of states on fractals: fractons. *J. Phys. Lett.* 1982;43; L625-L631.
- [30] Burioni R., Cassi D. Universal properties of spectral dimension. *Phys. Rev. Lett.* 1996;76; 1091-1093.
- [31] Saviot L., Duval E., Surotsev N., Jal J.F., Dianoux A.J. Propagating to nonpropagating vibrational modes in amorphous polycarbonate. *Phys. Rev. B.* 1999;60; 18-21.
- [32] Ben-Avraham D. Vibrational normal-mode spectrum of globular proteins. *Phys. Rev. B*

- 1993;47;14559.
- [33] Elber R., Karplus M. Low frequency modes in proteins: use of effective-medium approximation to interpret fractal dimension observed in electron-spin relaxation measurements. *Phys. Rev. Lett.* 1986;56:394-397.
 - [34] De Gennes P.G. *Scaling concepts in polymer physics.* Cornell University Press, Ithaca (1979).
 - [35] Bahar I., Atilgan A.R., Erman B. Direct evaluation of thermal fluctuations in proteins using a single-parameter harmonic potential. *Fold. Des.* 1997;2:173-181.
 - [36] Press W.H., Flannery B.P., Teukolsky S.A., Vetterling W.T. *Numerical recipes.* Cambridge University Press; Cambridge 1993.
 - [37] Kundu S., Melton J.S., Sorensen D.C., Phillips G.N.Jr. Dynamics of proteins in crystal: comparison of experiment with simple models. *Biophys. J.* 2002;34:723-732.
 - [38] Goldenfeld N. *Lectures on Phase Transitions and the Renormalization Group.* *Frontiers in Physics* 85 Addison-Wesley Publishing Company 1992.

PDB code	Length	\bar{d}	Error	$k_B T/\gamma$	Correl.
9RNT	104	1.62	0.05	1.657	0.474
1BVC	153	1.56	0.01	0.392	0.698
1G12	167	1.89	0.01	0.793	0.584
1AMM	174	1.71	0.06	0.003	0.720
4GCR	185	1.73	0.04	0.001	0.711
1KNB	186	1.88	0.01	1.104	0.699
1CUS	197	1.86	0.01	0.914	0.731
1IQQ	200	1.84	0.01	0.480	0.626
2AYH	214	1.86	0.02	0.539	0.773
1AE5	223	1.93	0.02	0.952	0.531
1LST	239	1.77	0.01	0.982	0.647
1A06	279	1.78	0.03	2.184	0.623
1NAR	289	1.81	0.01	0.602	0.696
1A48	298	1.72	0.01	0.664	0.549
1A3H	300	1.90	0.02	0.719	0.553
1SBP	309	1.74	0.02	0.641	0.757
1A5Z	312	1.74	0.01	2.111	0.574
1A1S	313	1.89	0.01	1.068	0.600
1ADS	315	1.79	0.03	0.500	0.687
1A40	321	1.90	0.04	0.524	0.546
1A54	321	1.86	0.03	0.601	0.516
1A0I	332	1.71	0.03	1.109	0.826
3PTE	347	1.79	0.01	0.366	0.840
1A26	351	1.82	0.01	1.369	0.635
1BVW	360	1.87	0.02	0.652	0.639
8JDW	360	1.94	0.01	1.293	0.607
7ODC	387	1.92	0.01	0.859	0.620
1OYC	399	1.93	0.01	1.056	0.697
1A39	401	1.97	0.01	1.113	0.656
16PK	415	1.82	0.03	0.630	0.590
1DY4	441	1.88	0.02	0.785	0.614
1BU8	446	1.95	0.01	0.859	0.632
1AC5	483	1.87	0.01	1.091	0.709
1LAM	484	1.97	0.01	0.488	0.583
1CPU	495	1.92	0.02	0.620	0.729
3COX	500	1.92	0.02	0.491	0.670
1A65	504	2.09	0.01	1.042	0.606
1SOM	528	2.00	0.02	1.585	0.653
1E3Q	532	1.97	0.01	1.577	0.623
1CRL	534	2.00	0.01	0.969	0.652
1AKN	547	1.87	0.01	1.737	0.667
1CF3	581	2.01	0.03	1.154	0.639
1EX1	602	2.01	0.03	1.193	0.598
1A14	612	2.10	0.09	0.865	0.524
1MZ5	622	2.02	0.04	0.750	0.705
1CB8	674	1.92	0.02	1.164	0.630
1HMU	674	1.92	0.02	0.907	0.684
1A47	683	2.02	0.04	0.646	0.529
1CDG	686	1.98	0.02	1.074	0.593
1DMT	696	1.96	0.02	1.204	0.536
1A4G	780	1.98	0.03	0.591	0.567
1HTY	1014	2.07	0.05	0.646	0.766
1KCW	1017	2.05	0.03	2.130	0.638
APP1	1021	1.93	0.02	0.805	0.576
1KEK	2462	2.07	0.05	1.263	0.730
1B0P	2462	2.08	0.09	0.319	0.810
1K83	3494	2.01	0.01	2.030	0.659
1I3Q	3542	1.97	0.01	2.435	0.758
1I50	3558	1.98	0.02	2.236	0.701

TABLE I: List of processed native protein structures from Brookhaven PDB, with their length, the corresponding spectral dimension estimated by GNM approach with cutoff $R_0 = 7\text{\AA}$, error on its determination, parameter $k_B T/\gamma$ and correlation ρ (4).

PDB code	Length	\bar{d}	Error	$k_B T/\gamma$	Correl.
9RNT	104	1.43	0.08	0.209	0.549
1BVC	153	1.36	0.02	0.186	0.626
1G12	167	1.61	0.04	0.412	0.599
1AMM	174	1.55	0.09	0.113	0.802
4GCR	185	1.48	0.09	0.002	0.689
1KNB	186	1.70	0.01	1.104	0.699
1CUS	197	1.71	0.03	0.453	0.693
1IQQ	200	1.57	0.02	0.199	0.625
2AYH	214	1.68	0.01	0.222	0.756
1AE5	223	1.66	0.02	0.396	0.537
1LST	239	1.59	0.01	0.441	0.707
1A06	279	1.52	0.01	0.907	0.621
1NAR	289	1.54	0.01	0.257	0.731
1A48	298	1.46	0.01	0.235	0.546
1A3H	300	1.71	0.01	0.342	0.414
1SBP	309	1.62	0.03	0.301	0.718
1A5Z	312	1.57	0.02	0.914	0.539
1A1S	313	1.70	0.01	0.523	0.643
1ADS	315	1.56	0.02	0.204	0.611
1A40	321	1.57	0.01	0.199	0.604
1A54	321	1.57	0.03	0.232	0.543
1A0I	332	1.60	0.01	0.492	0.799
3PTE	347	1.66	0.01	0.180	0.840
1A26	351	1.60	0.03	0.602	0.613
1BVW	360	1.73	0.02	0.297	0.527
8JDW	360	1.71	0.01	0.550	0.537
7ODC	387	1.54	0.01	0.301	0.586
1OYC	399	1.74	0.01	0.472	0.659
1A39	401	1.78	0.02	0.473	0.643
16PK	415	1.67	0.04	0.277	0.591
1DY4	441	1.84	0.02	0.357	0.535
1BU8	446	1.76	0.01	0.331	0.538
1AC5	483	1.60	0.02	0.482	0.646
1LAM	484	1.75	0.01	0.204	0.623
1CPU	495	1.67	0.01	0.235	0.546
3COX	500	1.72	0.01	0.202	0.571
1A65	504	1.86	0.03	0.421	0.701
1SOM	528	1.63	0.02	0.560	0.610
1E3Q	532	1.67	0.02	0.570	0.533
1CRL	534	1.81	0.01	0.448	0.648
1AKN	547	1.71	0.01	0.800	0.641
1CF3	581	1.73	0.05	0.473	0.560
1EX1	602	1.73	0.01	0.401	0.544
1A14	612	1.86	0.02	0.373	0.538
1MZ5	622	1.68	0.02	0.274	0.740
1CB8	674	1.66	0.02	0.425	0.627
1HMU	674	1.67	0.01	0.334	0.652
1A47	683	1.75	0.01	0.236	0.376
1CDG	686	1.76	0.01	0.402	0.454
1DMT	696	1.73	0.09	0.484	0.549
1A4G	780	1.99	0.09	0.244	0.554
1HTY	1014	1.70	0.07	0.267	0.739
1KCW	1017	1.82	0.01	0.918	0.581
APP1	1021	1.83	0.05	0.299	0.572
1KEK	2462	1.90	0.04	0.439	0.664
1B0P	2462	1.94	0.02	0.118	0.695
1K83	3494	1.90	0.04	0.781	0.631
1I3Q	3542	1.94	0.02	0.883	0.691
1I50	3558	1.96	0.05	0.816	0.653

TABLE II: List of processed native protein structures from Brookhaven PDB, with their length, the corresponding spectral dimension estimated by GNM approach with cutoff $R_0 = 6\text{\AA}$, error on its determination, parameter $k_B T/\gamma$ and correlation ρ (4).